Desalination and Water Treatment
www.deswater.com
doi: 10.1080/19443994.2015.1055814

57 (2016) 13295–13306
June

Taylor & Francis
Taylor & Francis Group

Preparation of a novel polymeric adsorbent and its adsorption of phenol in aqueous solution

Man Yang[a], Yun Huang[a,*], Qiudi Yue[a], Haijun Cao[b], Xing Li[a], Yuanhua Lin[a]

[a]*School of Materials Science and Engineering, Southwest Petroleum University, Chengdu 610500, Sichuan Province, PR China, Tel./Fax: +8602883037406; emails: yibinym2009@163.com (M. Yang), yunhuangswpu@163.com (Y. Huang), 573084311@qq.com (Q. Yue), 649418791@qq.com (X. Li), 1992605212@163.com (Y. Lin)*
[b]*Institute of Blood Transfusion, Chinese Academy of Medical Sciences, Chengdu 610052, Sichuan Province, PR China, Tel./Fax: +860285372370; email: huangyun982@163.com*

Received 21 December 2014; Accepted 22 May 2015

ABSTRACT

Phenol is one of the most representative pollutants in industrial wastewater, and the designation and development of a novel and valuable polymer adsorbent is one kind of outstanding method to treat phenol aqueous solution. In this study, a new polymeric adsorbent P(MMA-St-NMA) was synthesized and characterized. The affection of solution pH, initial concentration, time, and temperature on adsorption ability of the synthesized polymer adsorbent was then investigated. Based on the analysis of Fourier transform infrared spectra (FT-IR), ^{1}H NMR, ^{13}C NMR, X-ray diffraction, and differential scanning calorimetry, the polymer adsorbent was successfully synthesized. Through the obtained data, the optimum adsorption was achieved when pH was 6, initial concentration 6,000 mg/L, contact time 5 h, and the higher temperature. The adsorption kinetics was found to follow the pseudo-first-order kinetic model. The intra-particle diffusion analysis indicated that particle diffusion was involved in the adsorption process but it was not the only rate-limiting step. Adsorption isotherms of phenol were linearly correlated and found to be well represented by the Freundlich model. Thermodynamic parameters such as changes in the enthalpy (ΔH), free energy (ΔG), and entropy (ΔS) indicated that the adsorption phenol onto P(MMA-St-NMA) was an endothermic and spontaneous process.

Keywords: Phenol; Polymer adsorbent; Kinetics; Thermodynamics; Adsorption isotherm

1. Introduction

Water pollution, especially the industrial wastewater containing aromatic compounds, is one of the most urgent environmental problems. Phenol and its derivatives are common organic pollutants observed in effluents from various manufacturing operations such as paper, pesticides, dyes, petroleum refining, pharmaceutical, and in the synthesis of plastics [1]. Phenol can affect the liver, kidneys, lungs, and vascular system in human bodies through inhalation, ingestion, or skin contact. So it is necessary that wastewater containing phenol needs careful treatment before discharging into the receiving bodies of water.

Recently, various technical processes such as oxidation, biodegradation, solvent extraction, and adsorption have been proposed to remove phenolic

*Corresponding author.

pollutants from contaminated waters [2], among which adsorption is one of the most effective techniques in either laboratory or industry [3]. As a widely used adsorbent, activated carbon exhibits a satisfactory performance for phenol removal [4]. However, its wider application is restricted due to its high regeneration cost and high attrition rate. Bentonite is a naturally available clay mineral and can be used as a low-cost adsorbent, but its adsorption capacity is relatively poor. So the bentonite as an adsorbent needs further modification [5]. Cellulose can be used to adsorb aromatic pollutants by grafting of cyclodextrins on its surface, while the high cost of cyclodextrins and the low grafting yields on cellulose limit the large-scale development [6].

More recently, various polymeric adsorbents have been developed and implemented for phenol removal from aqueous solution. Amberlite XAD-4 is one of the best commercial polymeric adsorbents of the second generation styrene–divinylbenzene (St-DVB) copolymers for removing organic pollutants from aqueous solution [7,8], because the benzene ring of Styrene (St) and aromatic compounds can form π–π interaction, which is helpful to enhance the adsorption capacity. Xun Qiu, et al. used methyl methacrylate (MMA), n-butyl acrylate (BA), and St as monomer and synthesized a novel polymeric adsorbent by suspension polymerization. In this kind of adsorbent, the acrylic esters moieties from MMA provide the good affinity to phenol molecules by the formation of hydrogen bonds between ester groups and phenolic hydroxyl groups [9]. Besides, owing to the simple synthesis method and the easy operation, it has a potential practical value for the industrial application. N-methylol acrylamide (NMA) can be copolymerized with sodium p-styrenesulfonate (SSS) in aqueous phase or with MMA or butyl acrylate (BA) in oil phase [10,11]. The amide group and hydroxyl group in NMA can effectively form hydrogen bonding with phenolic hydroxyl group. These features contribute to phenol removal. And what's more, NMA is a functional monomer that can be dissolved in water, which makes the synthesized polymer adsorbent show hydrophilic to some extent. The performance improves the dispersion efficiency in aqueous solution, and ultimately increases the removal capacity of phenol.

Obviously, MMA, St, and NMA containing functional groups are all very useful components to deal with phenol in aqueous solution. So in the present research, choosing them as monomers to synthesize one new valuable polymer adsorbent P(MMA-St-NMA). We studied the adsorption behavior of phenol from aqueous solution with P(MMA-St-NMA); reviewed the effect of solution pH, initial concentration, contact time, and temperature; and discussed adsorption kinetics, isotherm, and thermodynamic of adsorbent for the adsorption of phenol.

2. Materials and methods

2.1. Materials

Polyvinyl alcohol (PVA), MMA, St, NMA, benzoyl peroxide (BPO), and phenol were purchased from Kelong Chemical Reagent (Chengdu, China). Hydrochloric acid and sodium hydroxide were obtained from Beijing Chemical Reagent Co. Ltd (Beijing, China) and were applied to adjust the solution pH. All reagents were of analytical purity grades and used without any further purification.

2.2. Preparation of the adsorbent

The polymer adsorbent was prepared via traditional suspension polymerization with MMA, St, and NMA as monomers. PVA was used as the dispersant and BPO as the initiator. Firstly, 1 g of PVA-1799 and 160 mL of deionized water were mixed in a 250-mL three-necked round bottom flask equipped with a reflux condenser and mechanical stirrer. Then, the temperature of the water bath was raised to 90˚C within 0.5 h so that the PVA dissolves adequately. After adding the initiator BPO (0.72 g), the monomer mixture (MMA 20 g, St 8 g, NMA 8 g) was added into the flask, and then, the reaction mixture was heated in the water bath at 75˚C for 4 h to obtain the target product. After cooling to room temperature, the polymeric beads were obtained and then washed with deionized water and ethanol three times, respectively. Finally, the products were dried under vacuum at 60˚C for 24 h.

2.3. Characterization

The FT-IR of the sample was recorded on a Nicolet 6700 spectrophotometer to check the functional groups of the material (KBr pellet) in the region of 4,000–400 cm^{-1}. The ^{1}H NMR and ^{13}C NMR spectrums of polymer were recorded using an AVII-400MHZ Nuclear magnetic resonance (NMR) spectrometer operated at 400 MHz, and deuterated acetone was used as the solvent. X-ray diffraction (XRD) measurement was tested by DX-2000 X-ray diffractometer for the polymer, and the scanning area was from 0˚ to 80˚. Differential scanning calorimetry analysis (DSC) was determined by an 822E DSC analysis instrument in air at a heating rate of 10˚C/min. The specific surface area, pore volume, and average pore diameter

were calculated by N_2 adsorption–desorption isotherms at 77 K using a F-sorb 3400 automatic surface area and porosity analyzer (Bei Jing Gold Spectrum Technology Corp. China). Before measuring these data, the samples were outgassed in vacuum for 8 h at 373 K on the degas port of the analyzer. The concentration of phenol in aqueous solution was analyzed by ultraviolet (UV) analysis performed on a UV-752 spectrophotometer (Shanghai Yoke Instrument Co. Ltd) with the wavelength at 270 nm.

2.4. Adsorption experiments

All batch experiments were carried out in 100-mL flasks. The effect of pH on phenol removal was studied by shaking 0.2 g of adsorbent and 25 mL of 1,000 mg/L phenol solution at pH 2–12. The adsorption process was kept for 24 h, in order to ensure the adsorption reached equilibrium. To adjust the pH, 1 mol/L HCl and 1 mol/L NaOH were used. The effect of initial concentration for phenol removal was determined by placing 0.2 g of adsorbent and 25 mL of phenol solution with desired concentrations (200–10,000 mg/L) and shaking for 24 h. The adsorption kinetics experiments were carried out by shaking 0.2 g of adsorbent and 25 mL of 1,000 mg/L phenol solution at pH 6 for different time intervals. The effect of temperature on phenol removal was studied by shaking 0.2 g of adsorbent and 25 mL of 1,000 mg/L phenol solution for 5 h. We set a list of temperatures from 25 to 50°C. The concentration of phenol in aqueous solution was determined with a UV–visible spectrophotometer at a specific wavelength 270 nm. The amount of adsorbed phenol was calculated by a mass balance between the initial and equilibrium concentrations. The equilibrium absorption (Q_e) of adsorbed phenol and the amount of adsorbed phenol (Q_t) at time t were calculated by the following formula, respectively.

$$Q_e = \frac{(C_o - C_e)V}{W} \quad (1)$$

$$Q_t = \frac{(C_o - C_t)V}{W} \quad (2)$$

where C_o is the initial phenol concentration (mg/L), C_e the residual phenol concentration at the equilibrium time (mg/L), C_t is the residual phenol concentration at the time t (mg/L), V *is* the volume of the solution (L), and W is the dosage of polymeric adsorbent (dry weight, g).

The calibration curve for aqueous solution of phenol was created by running different calibration standards (2, 4, 5, 8, 10, 12, 16, 20, 30, 50 mg/L). The absorbance values (A) were measured for each concentration (C) at λ_{max} = 270 nm by UV spectrometer. The values of concentration (C) were plotted against the corresponding A values, and the data points were linearly fitted. The resulted calibration equation was calculated as following: (R^2 = 0.999, R is the correlation coefficient).

$$A = 0.01404C + 0.00877 \quad (3)$$

3. Results and discussion

3.1. Characterizations of the P(MMA-St-NMA)

3.1.1. FT-IR analysis

To elucidate the presence of ester group, amide group, hydroxyl group, and benzene ring in the synthesized polymer, the infrared spectrum of the polymer was obtained and shown in Fig. 1. The two peaks at 3,548 and 3,410 cm^{-1} were assigned to the stretching vibration of –OH and –NH. The characteristic peak at 1,635 cm^{-1} in spectrum was attributed to –C=O stretching vibration of –CONH [12]. The bands observed at 1,727 and 1,138 cm^{-1} were assigned to the vibration of –C=O and –C–O–C [1], respectively. Besides, three peaks at 1,611, 752, and 702 cm^{-1} were due to the vibration of benzene ring [13,14]. While the characteristic peaks at 1,640–1,658 cm^{-1} assigned to the band of –C=C existed in each monomer disappeared in the spectrum. Owing to the above investigation, the target product was successfully synthesized by the suspension copolymerization.

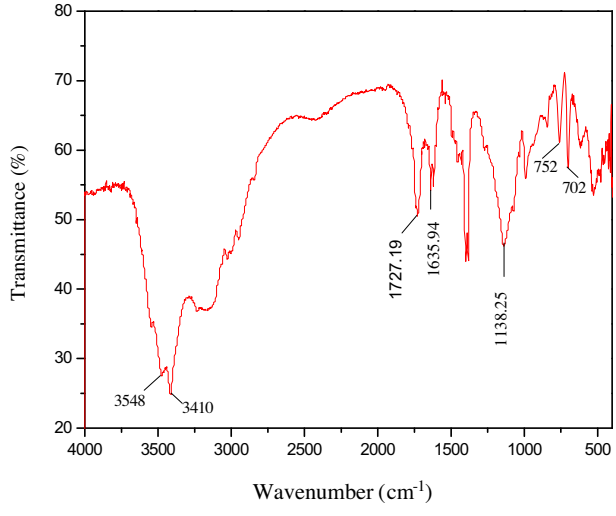

Fig. 1. FT-IR spectra of P(MMA-St-NMA).

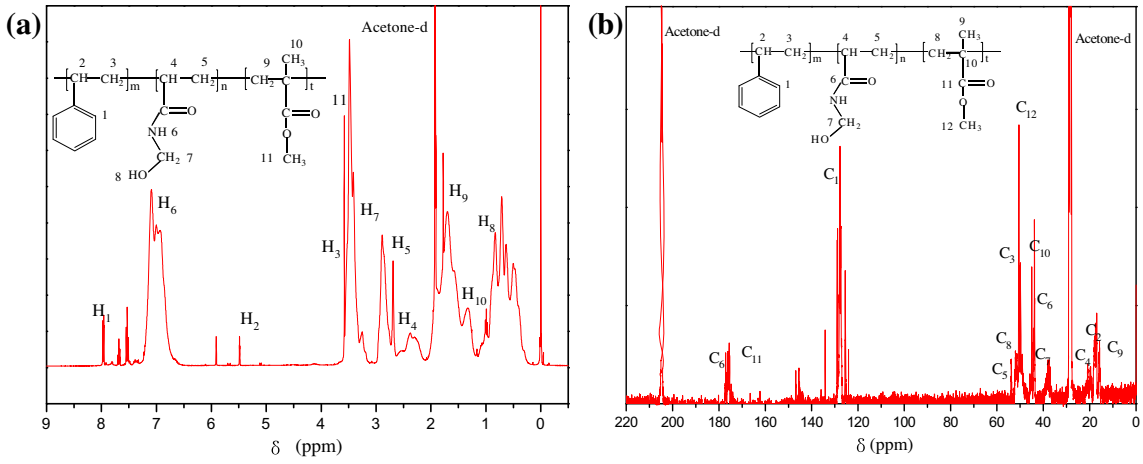

Fig. 2. NMR spectrum of P(MMA-St-NMA) ((a) ^{1}H NMR and (b) ^{13}C NMR).

3.1.2. ^{1}H NMR and ^{13}C NMR analysis

To further explain the structure of polymer, ^{1}H NMR and ^{13}C NMR of P(MMA-St-NMA) were illustrated in Fig. 2. In Fig. 2(a), the ^{1}H spectrum showed signals at 3.7, 2.6, 2.9, and 1.9 ppm for H_3, H_5, H_7, and H_9 respectively, evidence of the hydrogen protons of the methylene arising from the copolymerization. The signals at 1.6 and 3.7 ppm separately for H_{10} and H_{11} were from the hydrogen protons of the methyl, which proved the existence of the MMA [15]. The signals at 7.9 and 7.1 ppm indicated the presence of the benzene ring (H_1) and –NH–CO (H_6), respectively [16,17]. As it can be seen in Fig. 2(b), the ^{13}C NMR spectrum of the polymers showed the chemical shifts of the carbon [18]. The CH_2 group (C_3, C_5, and C_8) and CH group (C_2 and C_4) signals were evident at 20 and 55 ppm, respectively, whereas the signals at 16.9 and 52.6 ppm indicated the presence of the CH_3 (C_9 and C_{12}) in MMA. The signals at 132.5, 170.2, and 173.7 ppm for C_1, C_6, and C_{11} represented the evidence of the carbon of benzene ring, –NH–CO, and –COO, respectively. Thus, all of the above analysis about ^{1}H NMR and ^{13}C NMR corresponded well with the expected copolymer.

3.1.3. XRD analysis

To investigate the structure of the polymer, the result of XRD measurement was shown in Fig. 3. In the 2θ=43.6˚, 50.7˚, only two very weak peaks were observed for the polymer, so the structure of polymer was under the amorphous stage. This conclusion was consistent with the result of Yang [19].

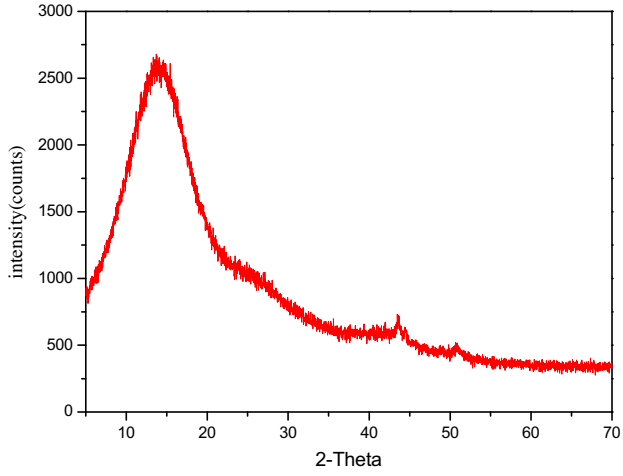

Fig. 3. XRD spectrum of P(MMA-St-NMA).

3.1.4. DSC analysis

The thermodynamic property of polymer was measured by the DSC and displayed in Fig. 4. Depending on some research results [20] and combining with this graphic, the glass transition temperature (T_g) was 120˚C. Owing to the amorphous structure, the polymer did not possess the obvious crystal melting adsorption peak.

According to the above characterizations, the synthesized polymeric adsorbent by suspension polymerization was the target product that we hoped to get. In order to acquire the adsorption capacity of the P (MMA-St-NMA) and investigate the related effect factors, we further discussed the adsorption studies in detail.

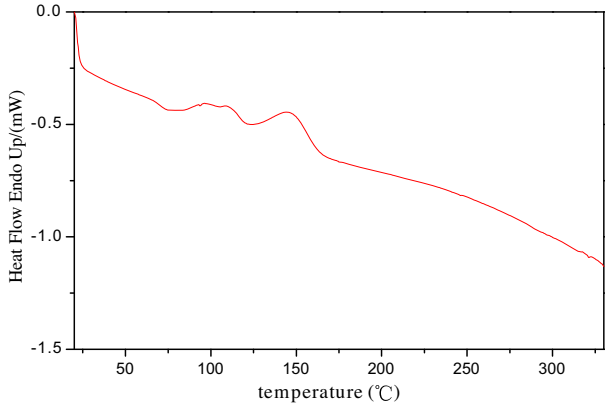

Fig. 4. DSC thermogram of P(MMA-St-NMA).

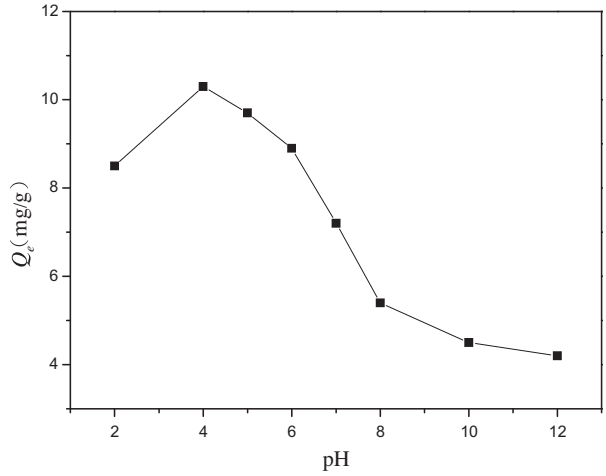

Fig. 5. Effect of solution pH on the phenol uptake onto P (MMA-St-NMA) at 298 K.

3.1.5. BET surface area analysis

The surface area is one of the most typical properties for evaluation of the adsorption performance of adsorbent. The physical characteristics of P(MMA-St-NMA) are determined and presented in Table 1. These physical properties of P(MMA-St-NMA) can provide reference for the subsequent discussed adsorption capacity of P(MMA-St-NMA) for phenol uptakes.

3.2. Adsorption studies

3.2.1. Effect of solution pH on adsorption

Adsorption of phenol onto P(MMA-St-NMA) was carried out in the pH range from 2.0 to 12.0 and represented in Fig. 5.

The adsorption capacity of phenol was higher in acid solution than that in alkaline solution as shown in Fig. 5. The reason is that in acid condition, a majority of phenol existed in protonation [21] was presented in Fig. 6(a) and produced hydroxyl bonding interaction with the adsorption binding sites such as –COO–, –CON–, and –OH groups and at the same time the electrostatic attraction binding sites benzene ring group (shown in Fig. 7). Obviously, in alkaline condition, the phenol molecule is easily dissociated into phenolate anion [21,22] in Fig. 6(b), the two kinds of interaction mentioned above completely disappeared.

Table 1
Physical properties of the studied P(MMA-St-NMA)

BET surface area (m^2/g)	Langmuir surface area (m^2/g)	Pore volume (cm^3/g)	Average pore diameter (nm)
0.11	0.15	0.27	10,139.34

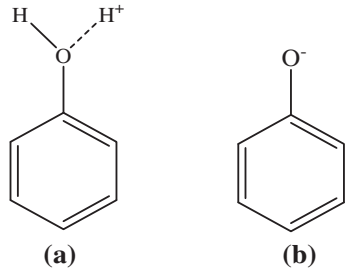

Fig. 6. The existence form of phenol ((a) the protonation of phenol and (b) the form of phenolate anion).

So when pH was beyond 7, the adsorption capacity of phenol decreased with pH.

But there was an interesting phenomenon when pH was below 7, when the value of pH was 4.0, the equilibrium adsorption (Q_e) was the biggest value and reached up to 10.3 mg/g. This can be explained as that when the pH value was below 4, there are enormous hydrogen ions H^+ from HCl solution used to adjust pH of phenol aqueous, and these hydrogen ions H^+ definitely occupy a large number of vacant adsorption binding sites in polymer adsorbent, which results to the phenol uptakes decrease. When pH was in the range of 4–7, a minority of phenol existed in molecule state and depended on the van der Waals force to be adsorbed onto the polymer adsorbent. The van der Waals force cannot endow polymer adsorbent with the same adsorption capacity as the hydroxyl bonding interactions do [23]. Therefore, the adsorption ability of the synthesized adsorbent achieved the highest point when pH was 4.

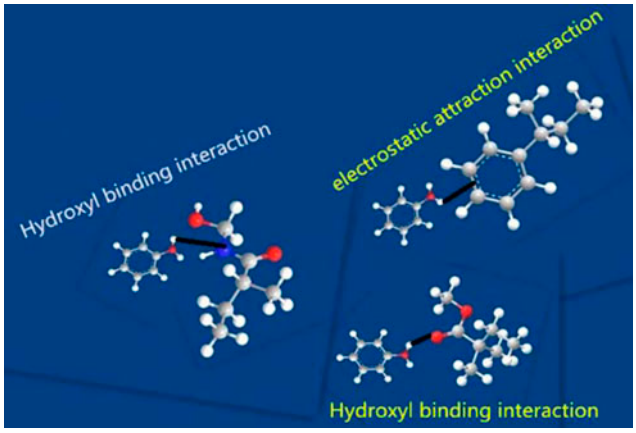

Fig. 7. The interaction between phenol and adsorbent.

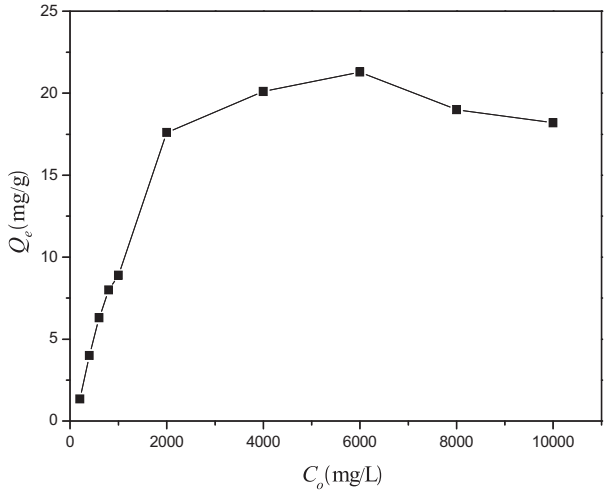

Fig. 8. Effect of initial concentration on the adsorption of phenol based on P(MMA-St-NMA).

Considering the actual industry conditions, the effluent containing phenol was influenced by the excessive acidic environment to some degree. Therefore, we decided to carry out the subsequent experiments at the pH 6.

3.2.2. Effect of initial concentration on adsorption

In order to investigate the effect of initial concentration, a series of initial concentrations as 200, 400, 600, 800, 1,000, 2,000, 4,000, 6,000, 8,000, and 10,000 mg/L were designed and the result was shown in Fig. 8.

From Fig. 8, when the initial concentration was below 6,000 mg/L, increasing the initial phenol concentration resulted in the phenol uptakes increase. At first, phenol uptake increased quickly when initial concentration was changed from 0 to 2,000 mg/L. Then, the rising trend became gentle while the initial concentration of phenol was from 2,000 to 6,000 mg/L. This can be explained as that the degree of increase of adsorption capacity in the exact concentration range is completely determined by the number of adsorption binding sites on adsorbent [24]. In the first low phenol concentration range, phenol molecule disperses sparsely in solution and just can occupy a small quantity of adsorption binding sites, so the adsorbent possesses better adsorption capacity. Whereas in the second middle phenol concentration, phenol separates densely and must hold a great deal of adsorption binding sites, so the adsorption ability of adsorbent grows slowly [15]. But when the initial concentration was over 6,000 mg/L, phenol uptake began to decrease. The reason is that hydrogen bonds exist some certain selectivity. In aqueous solution, water molecule is the donor/receptor of hydrogen bond and interacts with adsorbent and adsorbate, which partly inhibits the hydrogen bonding interaction between adsorbent and adsorbate. When the interaction with adsorbent and adsorbate is greater than that between adsorbate and water molecule in aqueous solution, the phenol uptake was predominated by hydrogen bonding. In addition, the intermolecular interaction of adsorbate also exists between hydrogen bonds, which greatly weaken the hydrogen bonding between adsorbate and adsorbent. When the initial concentration is below 6,000 mg/L, the hydrogen bonding interaction between adsorbent and phenol molecule is greater than the phenol molecule and water molecule, and the adsorption process is mainly affected by the former. When the initial concentration was over 6,000 mg/L, the former interaction was less than the latter. Owing to the higher concentration of phenol, the interaction between the phenol molecules was strengthened. It strongly hindered hydrogen bonding force between the adsorbate and adsorbent [25]. So with the initial concentration of phenol further increasing, the phenol uptake tended to decrease.

3.2.3. Effect of contact time and kinetics analysis

The effect of contact time on the phenol uptake on P(MMA-St-NMA) at different initial concentrations (800–2,000 mg/L) was depicted in Fig. 9. It was found that the rate of phenol uptake was rapid in the first 150 min and approximately 90% of adsorption was completed within 250 min for phenol. The amount of adsorption increased with contact time, and equilibrium was achieved within 300 min. This can be

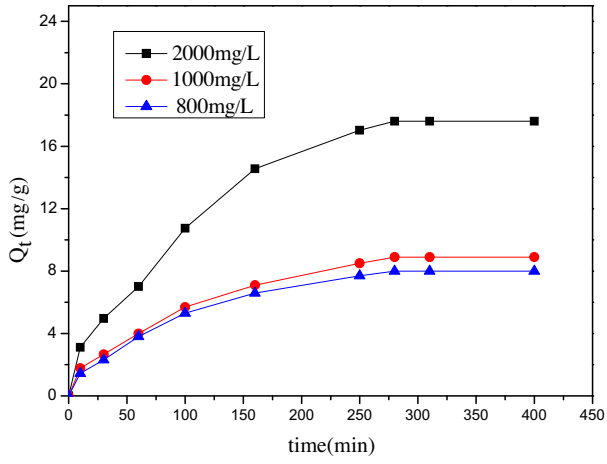

Fig. 9. Effect of contact time on the adsorption of phenol based on P(MMA-St-NMA).

attributed to a large number of vacant adsorption binding sites available for adsorption during the initial stage, and over time, the remaining vacant adsorption binding sites were increasingly difficult to be occupied due to repulsive forces between the solute molecules [15,26]. The high initial adsorption rate was due to the adsorption of phenol on the exterior surface of the adsorbent. When saturation was reached on the exterior surface, the phenol molecules migrated to the interior pores of adsorbent before uptake was achieved [25]. Eventually, the adsorption reached equilibrium.

Undoubtedly, the kinetic analysis is the useful and efficient method to illustrate the adsorption process. The widely used pseudo-first-order and pseudo-second-order model [15] were employed to fit the experimental data, respectively. The pseudo-first-order can be written as follows:

$$\ln\ (Q_e - Q_t) = \ln\ Q_e - k_1 t \tag{4}$$

where Q_t is the amount of adsorbed phenol at time t (mg/g) and Q_e is the equilibrium absorption of adsorbed phenol (mg/g). k_1 is the rate constant of pseudo-first-order model (min^{-1}). In the equation, ln (Q_e−Q_t) vs. t must show linear.

The pseudo-second-order model is given as:

$$\frac{t}{Q_t} = \frac{1}{k_2 Q_e^2} + \frac{t}{Q_e} \tag{5}$$

where k_2 is the rate constant of pseudo-second-order model (g/mg min). In the equation, t/Q_t vs. t also must show linear.

The corresponding fitting processes are shown in Fig. 10. They showed the fitted experimental data, using the pseudo-first-order model in Fig. 10(a) and the pseudo-second-order model in Fig. 10(b).

The first-order rate constant (k_1), the second-order rate constant (k_2), and correlation coefficient (R^2) obtained from the fitting linear plots for adsorption of phenol on P(MMA-St-NMA) were given in Table 2.

Q_e/exp is the experimental Q_e and Q_e/cal is the corresponding calculated Q_e according to the equation under study with best-fitted parameters.

The correlation coefficient R^2 in pseudo-first-order model was close to 1.0 than that in pseudo-second-order model as listed in Table 2. In addition, the experimental Q_e value also agreed with the calculated Q_e in pseudo-first-order model. So these results

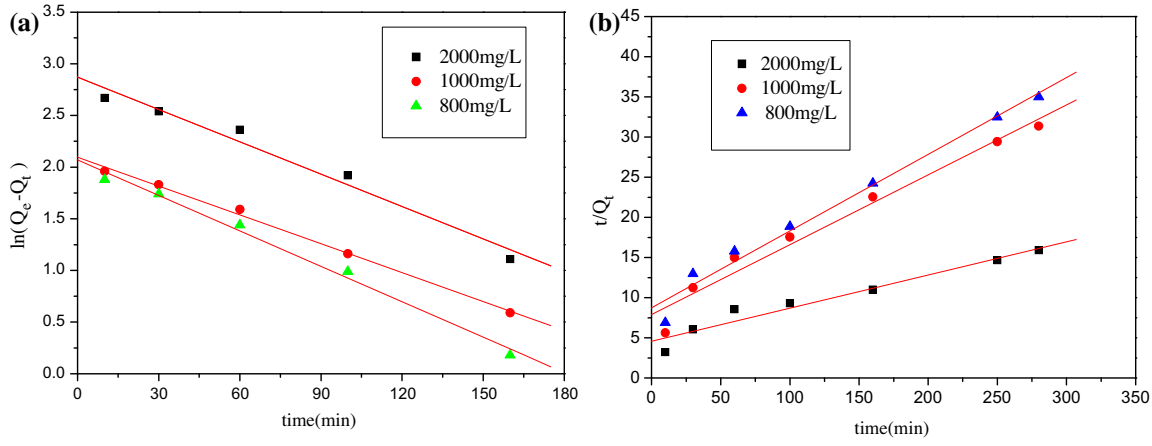

Fig. 10. The kinetic fitting curve for different initial phenol concentrations ((a) the fitting curve of pseudo-first-order model and (b) the fitting curve of pseudo-second-order model).

Table 2
The rate constants of adsorption kinetic model for different initial phenol concentrations on P(MMA-St-NMA)

		Pseudo-first-order			Pseudo-first-order		
C_o (mg/L)	Q_e/exp (mg/g)	Q_e/cal (mg/g)	k_1	R_1^2	Q_e/cal (mg/g)	k_2	R_2^2
800	8	7.90	0.0114	0.995	10.42	0.00105	0.990
1,000	8.9	8.20	0.0093	0.997	11.49	0.00096	0.985
2,000	17.6	17.54	0.0104	0.987	24.39	0.00037	0.975

indicated that the pseudo-first-order model did satisfactorily predict the kinetics of phenol adsorption onto the P(MMA-St-NMA).

In order to further investigate the mechanism of phenol adsorption and explain the reason that the adsorption process of phenol accorded with pseudo-first-order model, the following research was necessary and important. Usually, in the whole adsorption process, the adsorbate transported from the solution phase to the surface of the adsorbent particles occurs in several steps. The overall adsorption process may be controlled by any one of several steps, film or external diffusion, pore diffusion, surface diffusion and adsorption on the pore surface, or a combination of several steps [23]. Since the above kinetic models cannot identify the diffusion mechanism and rate-controlling step affected the kinetics of adsorption, the kinetic experimental data were further analyzed by the intra-particle diffusion model [15]. It is expressed as follows:

$$Q_t = k_d t^{1/2} + c \tag{6}$$

where k_d is the intra-particle diffusion rate (mg/g $\text{min}^{1/2}$), and c is a constant. The k_d and c were obtained by plotting Q_t vs. $t^{1/2}$.

The corresponding experimental data that were fitted by the intra-particle diffusion model showed in Fig. 11. According to the plots in Fig. 11, the values of k_3, c, and R_3^2 were calculated and were given in Table 3.

According to the intra-particle diffusion model, if intra-particle diffusion is the rate-limiting step, then Q_t vs. $t^{1/2}$ is linear and the data must pass through the origin (intercept = 0). On the other hand, if the plots are linear but do not pass through the origin, the rate of adsorption may be controlled by intra-particle diffusion together with other kinetic effects [22]. As can be seen from Fig. 11, the line did not pass through the origin. This indicated that particle diffusion was involved in the adsorption process but it was not the only rate-limiting step. Other mechanisms were involved [22,27]. It may be related to the

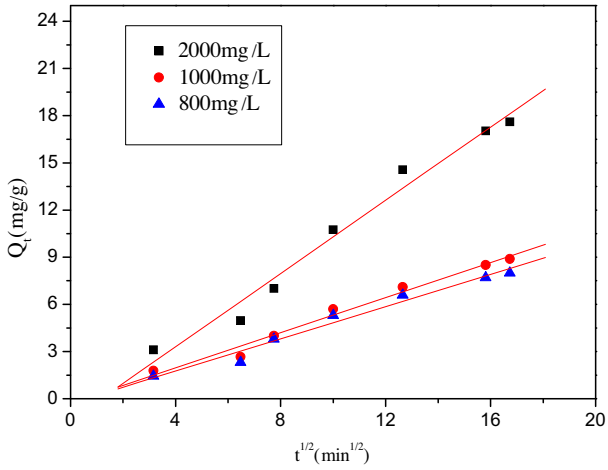

Fig. 11. Plot of intra-particle diffusion model for phenol uptake onto P(MMA-St-NMA) at different initial phenol concentrations.

Table 3
The kinetic fitting parameters of phenol adsorption onto P (MMA-St-NMA) for intra-particle diffusion model

Intra-particle diffusion			
C_o (mg/L)	k_d	c	R_3^2
800	0.512	−0.288	0.987
1,000	0.558	−0.260	0.991
2,000	1.163	−1.339	0.989

molecular size and the concentration of adsorbate, the affinity and pore size distribution of adsorbent. Finally, all of these impact factors made it reach equilibrium.

3.2.4. Adsorption isotherms

Equilibrium adsorption is usually described with an isotherm equation characterized by specific parameters, which expresses the surface property and affinity of adsorbent. In this study, adsorption of various initial phenol concentrations onto the adsorbent

(PMMA-St-NMA) were described with both Langmuir and Freundlich models.

The Langmuir adsorption isotherm assumes that monolayer adsorption onto a surface contains a finite number of adsorption binding sites and there is no interaction between the molecules adsorbed on the surface in solution [27]. The linear form of the Langmuir isotherm model [2] can be written as:

$$\frac{C_e}{Q_e} = \frac{C_e}{Q_m} + \frac{1}{K_L \cdot Q_m} \tag{7}$$

where Q_e is the equilibrium absorption of adsorbed phenol (mg/g), Q_m the theoretical monolayer capacity (mg/g), C_e the residual phenol concentration at equilibrium (mg/L), and K_L a constant. Fig. 12 described the result of the Langmuir adsorption isotherm.

The Freundlich isotherm supposes that the adsorption takes place at heterogeneous sites with nonuniform distribution of energy levels [27]. The Freundlich isotherm describes reversible adsorption and is not restricted to the formation of a monolayer. The logarithmic linear form of the Freundlich isotherm model [2] is given as:

$$\ln Q_e = \ln K_F + \frac{1}{n} C_e \tag{8}$$

where the parameter K_F (L/g) reflects the adsorption capacity and $1/n$ is the adsorption character. Fig. 13 indicated the result of the Freundlich isotherm.

Both the corresponding Langmuir and Freundlich equations parameters were calculated and listed in Table 4. First, the value of Q_m was below 0, so obviously, the Langmuir isotherm model did not describe the adsorption process. It was clear that the value of the correlation coefficient (R^2) in the Freundlich isotherm model was 0.952 and it was far more than that in the Langmuir isotherm model, which indicated that the Freundlich isotherm model can be used to describe the adsorption of phenol properly. Besides, the value of n in the Freundlich isotherm model was over 1, which demonstrated a favorable adsorption. At the same time, the value of K_F was 54.598, which also indicated the adsorption capacity of phenol onto adsorbent was very high.

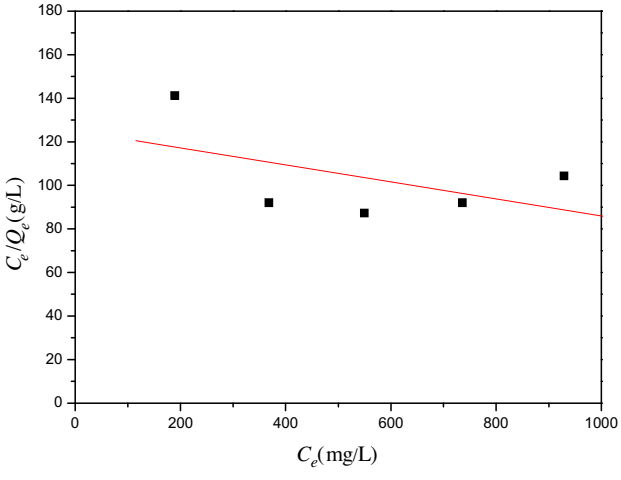

Fig. 12. The Langmuir adsorption isotherm of phenol based on P(MMA-St-NMA).

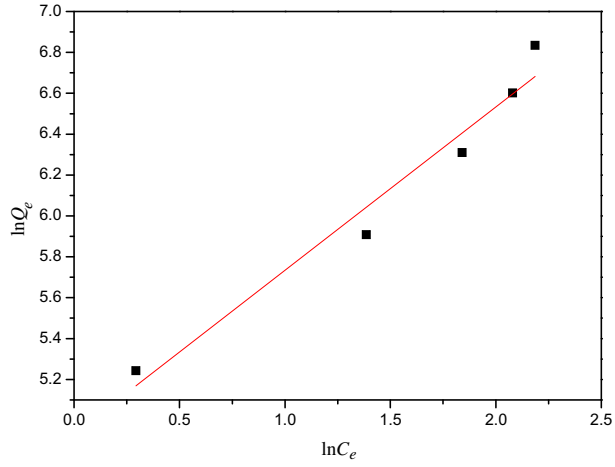

Fig. 13. The Freundlich adsorption isotherm of phenol based on P(MMA-St-NMA).

3.2.5. Effect of temperature and thermodynamics

Temperature is another impact factor that can affect the adsorption capacity of phenol. The effect of temperature on the adsorption of phenol onto P (MMA-St-NMA) was investigated in the temperature range of 25–55 ℃. The results are shown in Fig. 14.

According to most literatures [28,29], we knew adsorption was an exothermic process. But in the present research, on the contrary, as temperature rises, phenol uptakes increased gradually, which illustrated an endothermic process [25,30]. It can be explained that the diffusion speed and the adsorption binding sites of phenol increased with the temperature rising. Phenol molecules passed through the pore of the adsorbent easily and made phenol uptake increased. Besides, there existed hydrogen bonds between phenol molecule and water molecule before adsorbing. Besides, owing to the interactions of hydroxyl

Table 4
The parameters of adsorption isotherm for phenol adsorption based on P(MMA-St-NMA)

Langmuir			Freundlich		
K_L	Q_m	R_4^2	K_F	n	R_5^2
−0.00031	−25.601	0.0218	54.598	1.252	0.952

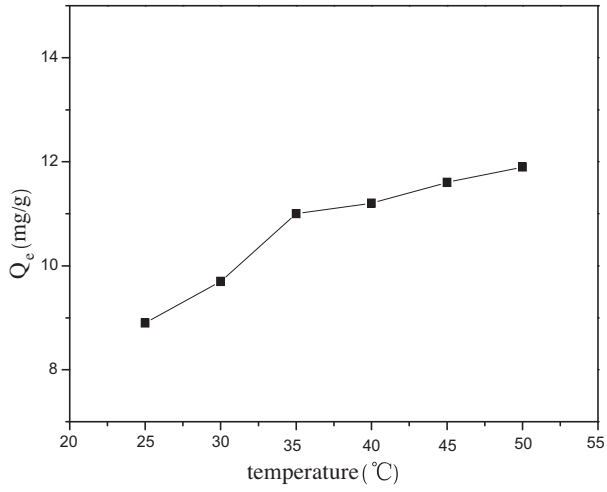

Fig. 14. Effect of temperature on the uptake of phenol by P (MMA-St-NMA).

bindings between phenol molecules and water molecules, these adsorbed phenol molecules need to be desorbed before adsorption, which is endothermic. Furthermore, the P(MMA-St-NMA) containing oxygen itself formed hydrogen bonds with water molecule. Some adsorption binding sites of the P(MMA-St-NMA) were occupied by water molecules. As a result, the water molecules must be desorbed from the P(MMA-St-NMA), which was also endothermic. Although phenol uptake onto adsorbent was exothermic, the heat was relatively small. It did not compensate the first two conditions. So it concluded that the adsorption of phenol onto P(MMA-St-NMA) was an endothermic process.

In environmental engineering practice, both energy and entropy factors must be considered in order to determine which process will occur spontaneously. So the adsorption thermodynamics parameters ΔH, ΔG, ΔS were calculated in our study.

Thermodynamic parameters such as the enthalpy change of adsorption (ΔH), change of free energy of adsorption (ΔG), and the entropy changes (ΔS) can be evaluated with the following equations [26]:

$$\ln C_e = -\ln K_o + \frac{\Delta H}{RT} \tag{9}$$

$$\Delta G = -nRT \tag{10}$$

$$\Delta S = \frac{\Delta H - \Delta G}{T} \tag{11}$$

where C_e is the equilibrium concentration of phenol (mg/L) and was obtained from the equilibrium state at a definite initial phenol concentration (1,000 mg/L) at different temperatures. T is the absolute temperature (K), ΔH the isosteric enthalpy change of adsorption (kJ/mol), R the ideal gas constant (8.314 J/mol K), K_o a constant, n the Freundlich exponent, ΔG the adsorption free energy (kJ/mol), and ΔS is the adsorption entropy change (J/mol K).

The enthalpy change (ΔH) value was determined from the slope of the linear plot of $\ln C_e$ vs. $1/T$ (shown in Fig. 15). According to the fitting curve, the fitted equation was expressed as:

$$\ln C_e = 503.09/T + 5.15 \tag{12}$$

The linear relation coefficient R^2 was 0.989, which illustrated the liner fitting of equation was well. So the ΔH value was 4.183 kJ/mol, the ΔG value obtained from Eq. (10) was −3.09 kJ/mol at 298 K. Then, from Eq. (11), the ΔS value was 24.41 J/mol K at 298 K.

From the above calculated results, the positive adsorption enthalpies indicated an endothermic process. And the value of ΔH was less than 40 kJ/mol

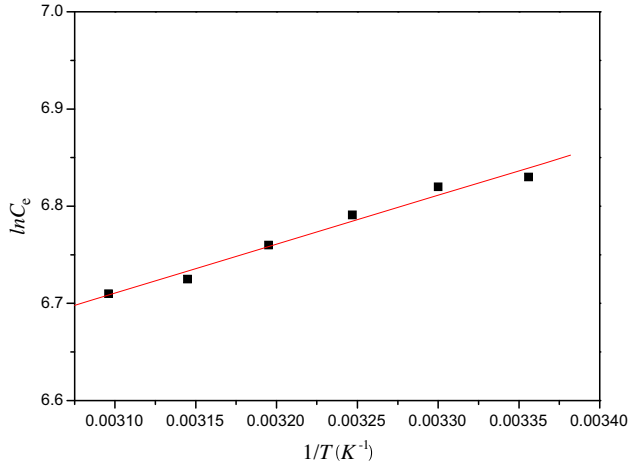

Fig. 15. Thermodynamics plots of adsorption.

and indicated a physical adsorption process [28]. Negative Gibbs free energy change demonstrated the adsorption of phenol with the adsorbent carried out spontaneously [28]. Besides, the positive value of the standard entropy (ΔS) reflected the adsorption was a process of entropy and the randomness of system was increased [25]. It can be explained that phenol molecules were much bigger than the water molecules. On the one hand, phenol molecules were adsorbed onto the adsorbent, the randomness of system was reduced. On the other hand, water molecules were desorbed from the adsorbent, which led to the increase of randomness of the system. The number of the desorbed water molecules was more than the adsorbed phenol molecules. So the final result was a process of entropy production.

4. Conclusions

In this work, we successfully prepared a novel polymeric adsorbent of P(MMA-St-NMA) by suspension polymerization. The adsorption results showed that the obtained polymer was a potential adsorbent for phenol removal from aqueous solution. The optimum adsorption was achieved when pH was 6, initial concentration 6,000 mg/L, contact time 5 h, and the higher temperature. The adsorption followed the pseudo-first-order kinetic model. The particle diffusion was not the only rate-limiting step. Adsorption isotherms found to be well represented by the Freundlich model. Thermodynamic research indicated that the adsorption process was endothermic and spontaneous.

All adsorption investigation presented that the phenol removal from aqueous solution using the synthesized adsorbent expressed the very strong regularity, which implied that the polymer did not possess the excellent adsorption ability but undoubtedly was one kind of potential adsorbent in practical application. The limited adsorption ability is the result of very smooth surface of adsorbent, so in the future work, the rough extent enhancement of adsorbent surface using the experimental technology will be the research key point.

Acknowledgements

The authors gratefully acknowledge the financial support from the Specialized Research Fund for the Doctoral Program of Higher Education of China (20115121120005) and the Innovative Research Team of Sichuan Provincial Education Department.

References

[1] T. Saitoh, Y. Sugiura, K. Asano, M. Hiraide, Chitosan-conjugated thermo-responsive polymer for the rapid removal of phenol in water, React. Funct. Polym. 69 (2009) 792–796.
[2] B.J. Pan, B.C. Pan, W.M. Zhang, Q.R. Zhang, Q.X. Zhang, S.R. Zheng, Adsorptive removal of phenol from aqueous phase by using a porous acrylic ester polymer, J. Hazard. Mater. 157 (2005) 293–299.
[3] B.C. Pan, X. Zhang, W.M. Zhang, J.Z. Zheng, B.J. Pan, J.L. Chen, Q.X. Zhang, Adsorption of phenolic compounds from aqueous solution onto a macroporous polymer and its aminated derivative: Isotherm analysis, J. Hazard. Mater. 121 (2005) 233–241.
[4] B. Ozkaya, Adsorption and desorption of phenol on activated carbon and a comparison of isotherm models, J. Hazard. Mater. 129 (2006) 158–163.
[5] S. Al-Asheh, F. Banat, L. Abu-Aitah, Adsorption of phenol using different types of activated bentonites, Sep. Purif. Technol. 33 (2003) 1–10.
[6] E. Vismara, L. Melone, G. Gastaldi, C. Cosentino, G. Torri, Surface functionalization of cotton cellulose with glycidyl methacrylate and its application for the adsorption of aromatic pollutants from wastewaters, J. Hazard. Mater. 170 (2009) 798–808.
[7] I. Dobrevsky, A. Zvezdov, An application of mercury intrusion to explain some peculiarities in the behaviour of the polymeric adsorbent Amberlite XAD-4 during the process of adsorption of phenol from aqueous solutions, Powder Technol. 29 (1981) 205–208.
[8] A.M. Li, Q.X. Zhang, J.L. Chen, Z.H. Fei, C. Long, W.X. Li, Adsorption of phenolic compounds on Amberlite XAD-4 and its acetylated derivative MX-4, React. Funct. Polym. 49 (2001) 225–233.
[9] X. Qiu, N.J. Li, X.S. Ma, S. Yang, Q.F. Xu, H. Li, J.M. Lu, Facile preparation of acrylic ester-based cross-linked resin and its adsorption of phenol at high concentration, J. Environ. Chem. Eng. 2 (2014) 745–751.
[10] H. Yin, C. Lee, W. Chiu, Preparation of thermally curable conductive films PEDOT: P(SS-NMA) and their performances on weather stability and water resistance, Polymer 52 (2011) 5065–5074.
[11] H. Kolya, S. Das, T. Tripathy, Synthesis of Starch-g-Poly-(N-methylacrylamide-co-acrylic acid) and its application for the removal of mercury(II) from aqueous solution by adsorption, Eur. Polym. J. 58 (2014) 1–10.
[12] C. Păcurariu, G. Mihoc, A. Popa, S.G. Muntean, R. Ianoş, Adsorption of phenol and p-chlorophenol from aqueous solutions on poly (styrene-co-divinylbenzene) functionalized materials, Chem. Eng. J. 222 (2013) 218–227.
[13] M. Sobiesiak, B. Gawdzik, A.M. Puziy, O.I. Poddubnaya, Polymer-based carbon adsorbents obtained from copolymer of 4,4´-bis(maleimidodiphenyl)methane and divinylbenzene for use in SPE, Chromatographia 64 (2006) 1–7.
[14] S.A. Bortolato, K.E. Thomas, K.M. McDonough, R.W. Gurney, D.M. Martino, Evaluation of photo-induced crosslinking of thymine polymers using FT-IR spectroscopy and chemometric analysis, Polymer 53 (2012) 5285–5294.

[15] A.H. Al-Muhtaseb, K.A. Ibrahim, A.B. Albadarin, O. Ali-khashman, G.M. Walker, M.N. Ahmad, Remediation of phenol-contaminated water by adsorption using poly(methyl methacrylate) (PMMA), Chem. Eng. J. 168 (2011) 691–699.
[16] J.M. Li, X.G. Meng, C.W. Hu, J. Du, Adsorption of phenol, *p*-chlorophenol and *p*-nitrophenol onto functional chitosan, Bioresour. Technol. 100 (2009) 1168–1173.
[17] J.E. dos Santos, E.R. Dockal, É.T.G. Cavalheiro, Synthesis and characterization of Schiff bases from chitosan and salicylaldehyde derivatives, Carbohydr. Polym. 60 (2005) 277–282.
[18] Q.H. Liu, C.M. Li, L. Wei, M. Shen, Y.F. Yao, B.W. Hu, Q. Chen, The phase structure, chain diffusion motion and local reorientation motion: ^{13}C Solid-state NMR study on the highly-crystalline solid polymer electrolytes, Polymer 55 (2014) 5454–5459.
[19] C.C. Yang, Chemical composition and XRD analyses for alkaline composite PVA polymer electrolyte, Mater. Lett. 58 (2003) 33–38.
[20] J.L. de la Fuente, M.R. Ruiz-Bermejo, C.M. Menor-Salván, S.O. Osuna-Esteban, Thermal characterization of HCN polymers by TG-MS, TG, DTA and DSC methods, Polym. Degrad. Stab. 96 (2011) 943–948.
[21] F.Q. An, B.J. Gao, X.Q. Feng, Adsorption mechanism and property of novel composite material PMAA/SiO_2 towards phenol, Chem. Eng. J. 153 (2009) 108–113.
[22] J.J. Yin, R. Chen, Y.S. Ji, C.D. Zhao, G.H. Zhao, H.X. Zhang, Adsorption of phenols by magnetic polysulfone microcapsules containing tributyl phosphate, Chem. Eng. J. 157 (2011) 466–474.
[23] V.C. Srivastava, I.D. Mall, I.M. Mishra, Characterization of mesoporous rice husk ash (RHA) and adsorption kinetics of metal ions from aqueous solution onto RHA, J. Hazard. Mater. 134 (2006) 257–267.
[24] X.L. Jin, Y.F. Li, C. Yu, Y.X. Ma, L.Q. Yang, H.Y. Hu, Synthesis of novel inorganic-organic hybrid materials for simultaneous adsorption of metal ions and organic molecules in aqueous solution, J. Hazard. Mater. 198 (2011) 247–256.
[25] I.A. Tan, A.L. Ahmad, B.H. Hameed, Adsorption isotherms, kinetics, thermodynamics and desorption studies of 2,4,6-trichlorophenol on oil palm empty fruit bunch-based activated carbon, J. Hazard. Mater. 164 (2009) 473–482.
[26] F.Q. Liu, M.F. Xia, S.L. Yao, A.M. Li, H.S. Wu, J.L. Chen, Adsorption equilibria and kinetics for phenol and cresol onto polymeric adsorbents: Effects of adsorbents/adsorbates structure and interface, J. Hazard. Mater. 152 (2008) 715–720.
[27] X.J. Hu, J.S. Wang, Y.G. Liu, X. Li, G.M. Zeng, Z.L. Bao, X.X. Zeng, A.W. Chen, F. Long, Adsorption of chromium(VI) by ethylenediamine-modified cross-linked magnetic chitosan resin: Isotherms, kinetics and thermodynamics, J. Hazard. Mater. 185 (2011) 306–314.
[28] X.L. Guo, J. Wang, Y. Wang, Research of phenols adsorption from simulated coal gasification wastewater by resin, Procedia Environ. Sci. 12 (2012) 152–158.
[29] M. Raoov, S. Mohamad, M.R. Abas, Removal of 2,4-dichlorophenol using cyclodextrin-ionic liquid polymer as a macroporous material: Characterization, adsorption isotherm, kinetic study, thermodynamics, J. Hazard. Mater. 263 (2013) 501–516.
[30] Y. Ma, Q. Zhou, S.C. Zhou, W. Wang, J. Jin, J.W. Xie, A.M. Li, C.D. Shuang, A bifunctional adsorbent with high surface area and cation exchange property for synergistic removal of tetracycline and Cu^{2+}, Chem. Eng. J. 258 (2014) 26–33.